Field Evaluation of Energy Balance Simulation of Surface Soil Temperatures

R. M. Aiken, D. C. Nielsen, M. F. Vigil and L. R. Ahuja

Introduction

Surface crop residues help stabilize soils by reducing soil water loss, reducing the erosive force of wind and shielding the soil from a reduced number of saltating particles. Evaporation reduction by crop residues results from shading and protection from drying winds (Van Doren and Allmaras, 1978). Standing stems reduce the wind energy available for momentum transfer at the soil surface (Hagan and Armbrust, 1994; Lyles and Allison, 1976; Raupach, 1992).

The geometry of crop residues alters the surface microclimate, impacting the degree of soil protection and water conservation. Strips of partial mulch cover increased preplant soil warming (Bristow and Abrecht, 1989), while standing stems increased crop water use by increasing the transpiration fraction of total evaporation (Lascano et al., 1994). Vertical crop stems trapped more snow than horizontal stems (Nielsen and Hinkle, 1994). Decomposition of surface residues and the persistence of standing stems change with climate, soil environment, and management conditions (Steiner et al., 1994; Vigil, 1995), but impacts on soil water dynamics are less well understood.

Soil and crop management decisions are supported by accurate wind erosion prediction systems. Knowledge of crop residue geometry effects on heat and water exchange processes at the soil surface can extend the applicability of soil water balance modules for decision support. Our objectives were to determine 1) the seasonal changes in crop residue geometry, 2) effects of residue on soil water recharge efficiency, and 3) the predictive accuracy of PENFLUX, a numerically reduced soil-residue energy boundary condition module, that is compatible with the USDA-ARS Root Zone Water Quality Model.

Methods and Materials

Field Studies

We quantified soil and residue microclimate conditions following the 1995 harvest of wheat (*Triticum aestivum*), proso millet (*Panicum miliaceum*), corn (*Zea mays*) , and sunflower (*Helianthus annuus*) under no till management at the ARS Central Great Plains Research Station located 7 km E of Akron, CO (40º N, 103º W, 1400 m elev.). Stubble mulch tillage of wheat (wheat_SM) was included for comparison with wheat_NT(no tillage). The study site was located on a level Weld silt loam (fine montmorillonitic, mesic Aridic Paleustolls) soil. We deployed an automated data acquisition system to measure incident and reflected horizontal solar and net irradiance; air, residue, and soil temperatures; humidity; and wind speed. Measurements were made once each minute and averaged at hourly intervals.   Repeated measurements of standing

stems (height, frequency, and diameter) and surface residue cover (by 100 point line intercept) quantified seasonal change in the geometry of crop residues (Table 1). The silhouette factor, or stem area index (SAI) is the vertical projected area of standing stems found in a unit area of land surface, e.g. the product of stem diameter, stem height and stem population. Sequential harvest of pre-weighed wheat, corn and millet residues, secured in litter bags or 6.3 mm hardware mesh,

Table 1. Residue Architecture and Site Conditions, Spring 1996				
Crop Residue*	Residue Cover (m^2/m^2)	Stem Area Index (m^2/m^2)	Stem Height (m)	Soil Water (0 to 0.3 m, m^3/m^3)
Wheat_SM	0.10	0.010	0.05	0.29
Wheat_NT	0.85	0.306	0.23	0.34
Millet_NT	0.57	0.051	0.11	0.34
Corn_NT	0.39	0.034	0.38	0.35
Sunflower_NT	0.15	0.024	0.59	0.29

*Stubble mulch (SM) and no till (NT) residue management systems

provided direct measure of residue mass loss. Wind velocity profiles were obtained, under neutral stability conditions, over fields with consistent residue cover for at least 200 times the height of the top anemometer (2.4 m), assuring measurements represent convective conditions well adjusted to soil-residue geometries. Stored soil water was determined by time-domain reflectometry (0 to 0.3 m) and by neutron thermalization (0.3 to 1.8 m). We computed soil water recharge efficiency as the ratio of change in soil water to cumulative precipitation over a time interval.

Simulation Model

A diagrammatic representation of energy balance equations for soil and residue sub-layers (Aiken et al., 1997) is shown in Figure 1. Convective transfer coefficients correspond to sensible and latent heat flux densities above the displacement plane associated with standing residues ($r_{a(a)}$, $r_{a(r)}$, H, λE), within the residue layer ($r_{b(r)}$, $r_{s(r)}$, H_r, λE_r), and above the surface soil layer ($r_{h(r)}$, $r_{v(r)}$, $r_{s(s)}$, H_s, λE_s). Fluxes emanating from soil and residue surfaces are referenced to ambient conditions within the flat residue sub-layer. Net irradiance at the residue ($R_{n(r)}$) and soil ($R_{n(s)}$) surfaces are important driving variables partitioned in a transmission scheme based on the principle of superposition (Farahani and DeCoursey, 1998). Ambient temperature and vapor pressure conditions are specified boundary conditions at the reference height ($T_{a(a)}$ and $e_{a(a)}$) and state conditions within the residue sub-layer ($T_{a(r)}$ and $e_{a(r)}$). State conditions are also specified for the evaporative sources of surface residues (T_r and e_r) and the soil surface layer (T_s and e_s). Soil temperature is specified at the lower boundary of a soil slab, T_z. Soil heat flux, G, is a

significant source/sink term computed from soil thermal gradients and time change, using soil thermal conductivity ($k_{t(s)}$) and heat capacity (C_s). Governing equations for soil and residue layer temperatures are shown. For energy-limiting evaporation, we define γ_s^* as $\gamma(r_{s(s)} + r_{v(r)})/r_{h(r)}$, where γ is the psychrometric constant, and compute surface soil source temperature, T_s, as

$$T_s = T_{a(r)} + \frac{r_{h(r)}}{C_a}\frac{\gamma_s^*\left(R_{n(s)}-G\right)}{\left(\Delta+\gamma_s^*\right)} - \frac{\delta e_{a(r)}-\delta e_s}{\Delta+\gamma_s^*} \tag{1}$$

where the independent terms represent soil warming due to radiation absorbed under saturation water vapor pressures and soil cooling due to gradients in water vapor saturation deficits. Defining γ_r^* as $\gamma(r_{s(r)} + r_{b(r)})/(r_{b(r)})$, we compute surface residue temperature for energy-limiting evaporation by

$$T_r = T_{a(r)} + \frac{r_{b(r)}}{C_a}\frac{\gamma_r^* R_{n(r)}}{\left(\Delta+\gamma_r^*\right)} - \frac{\delta e_{a(r)}-\delta e_r}{\Delta+\gamma_r^*} \tag{2}$$

We use a Newton-Raphson iterative solution for the coupled set of equations (Bristow, 1987), subject to environmental driving variables and system parameters. The resulting terms are passed as boundary conditions to soil heat and water modules.
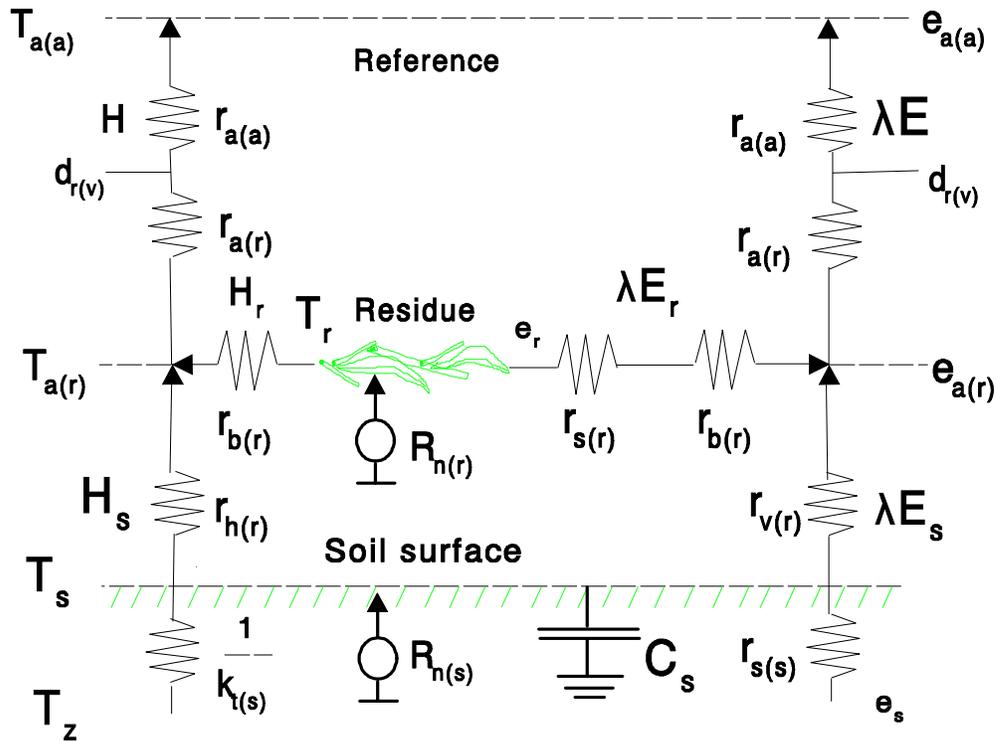
Figure 1. An electric resistance analog of heat and vapor exchange in a soil-residue system as simulated by the PENFLUX energy balance module.

Results and Discussion

Field Observations

Soil water recharge efficiency, the ratio of change in soil water to cumulative rainfall, is a water management performance measure for cropping systems. Repeated measure of soil water profiles under wheat_NT and wheat_SM management illustrate residue and tillage effects on soil water recharge efficiency (Figure 2.). Recharge efficiency averaged 0.93 for wheat_NT, but 0.64 for wheat_SM from April 22 through May 30. Thereafter, recharge efficiency dropped for both systems. Loss of rainfall is attributed to runoff, drainage, and evaporation for wheat_NT, as the 1.8 m soil profile reached capacity on June 3. Loss of rainfall for wheat_SM is attributable to runoff and evaporation, as the wetting front failed to reach the lowest (1.8 m) measurement depth. Retaining wheat stubble on the surface increased soil water recharge efficiency relative to stubble mulch tillage. Recharge efficiency decreased for both systems when profile water holding capacity was reached (wheat_NT) or evaporation and runoff exceeded precipitation (wheat_SM).
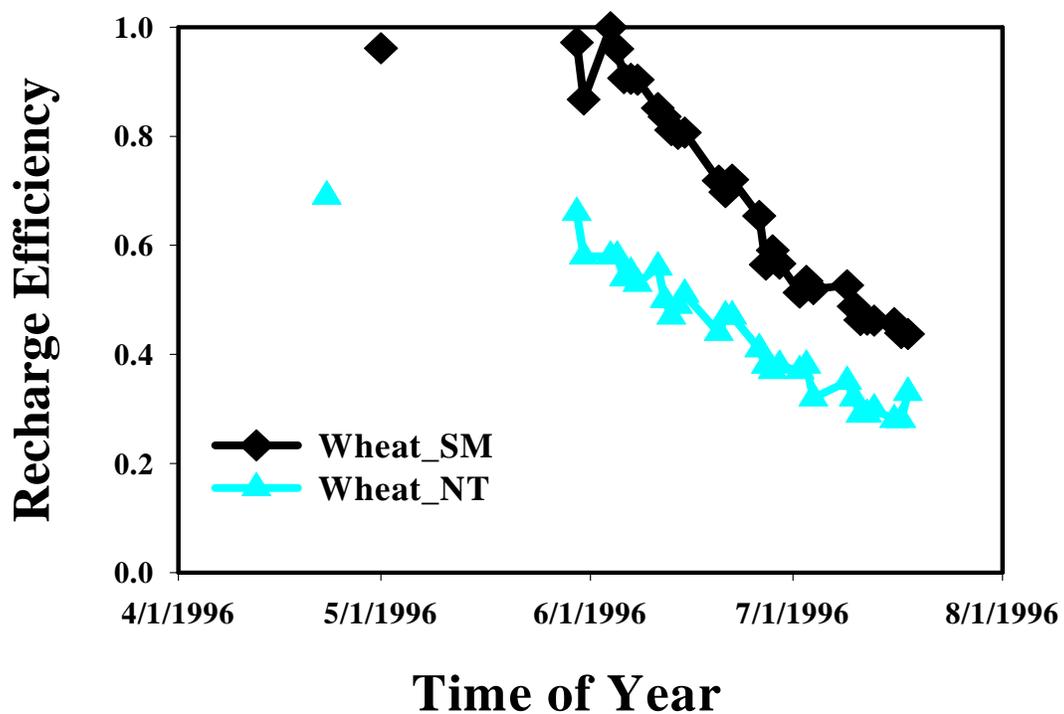
Figure 2. Soil water recharge efficiency, the ratio of change in soil water to cumulative rainfall for wheat_NT and wheat_SM systems.

Standing stems aid soil and water conservation by reducing turbulent mixing and the erosive force of near-surface winds. Wind speeds decreased with wheat stubble, which is taller than millet and has greater silhouette area than corn. These results show effects of residue geometry on wind conditions (Figure 3). Aerodynamic drag of standing stems absorb wind momentum. Quantitative knowledge of residue geometry effects on drag partitioning can improve predictive accuracy of surface energy balance and wind erosion modules.
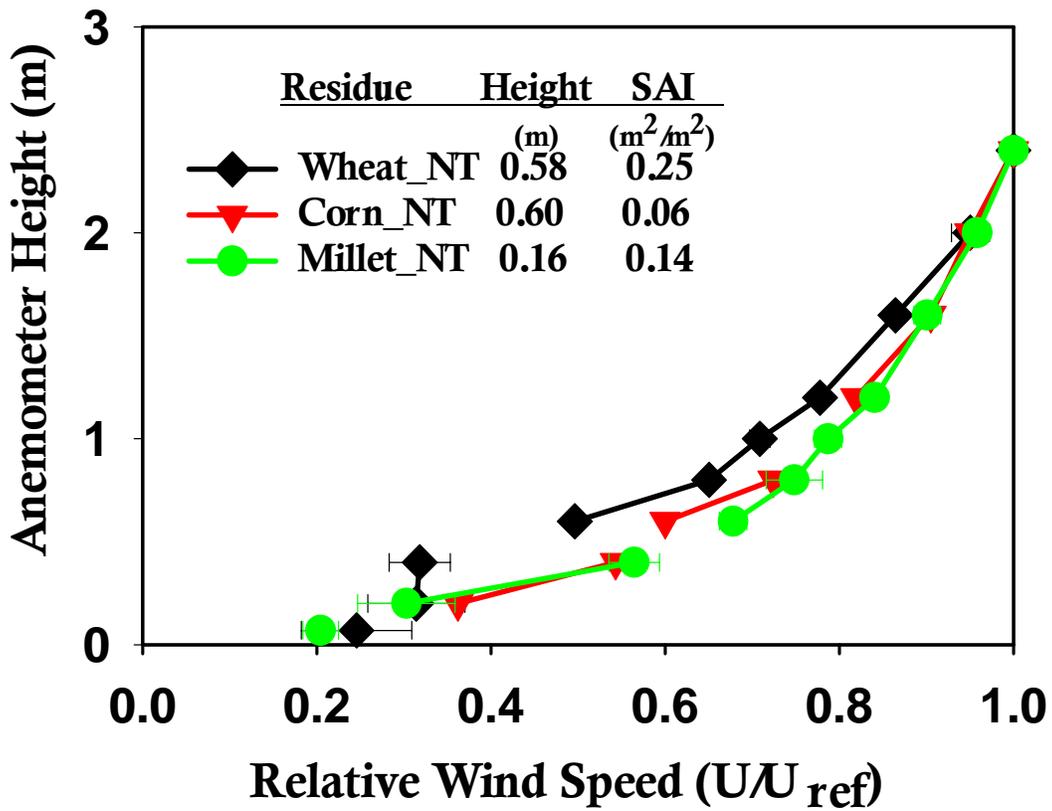
Figure 3. Relative wind speed profiles above corn_NT, millet_NT, and wheat_NT standing stems differing in height and stem area index (SAI); standard deviation is indicated for each measurement height.

Residue geometry (soil cover, stem area index) changed through a 14-month fallow period for wheat, corn and millet residues. Decomposition activity of surface organisms and mechanical action of wind alter the architecture of surface residues. The timing and magnitude of these dynamic processes are illustrated in Figure 4. Recovery of pre-weighed, surface-applied residues (Fig. 4a) demonstrates that surface residues are preserved during dry fall and cold winter conditions. Similar rates of mass loss for wheat, corn and millet residues indicate that spring moisture and soil warming favor decomposition.

The stem area index of standing stems declined as a near-linear function of time for wheat_NT, corn_NT and millet_NT residues (Fig. 4b), a consequence of fallen stems. Previous studies, of longer duration, show accelerated stem fall after an initial near-linear rate (Steiner et al., 1994; Vigil and Sparks, 1995). We hypothesize that stem fall accelerates with decomposition because the stem base weakens as roots decay; consequently, lower wind speeds are capable of knocking over standing stems.

Soil cover provided by millet and corn stubble diminished throughout the winter and spring (Fig. 4c). We attribute the overwinter loss to mechanical action of wind, as mass loss by decomposition was negligible during this period (Fig. 4a). Fallen wheat stems replenish the soil cover provided by flat residues.

a

b
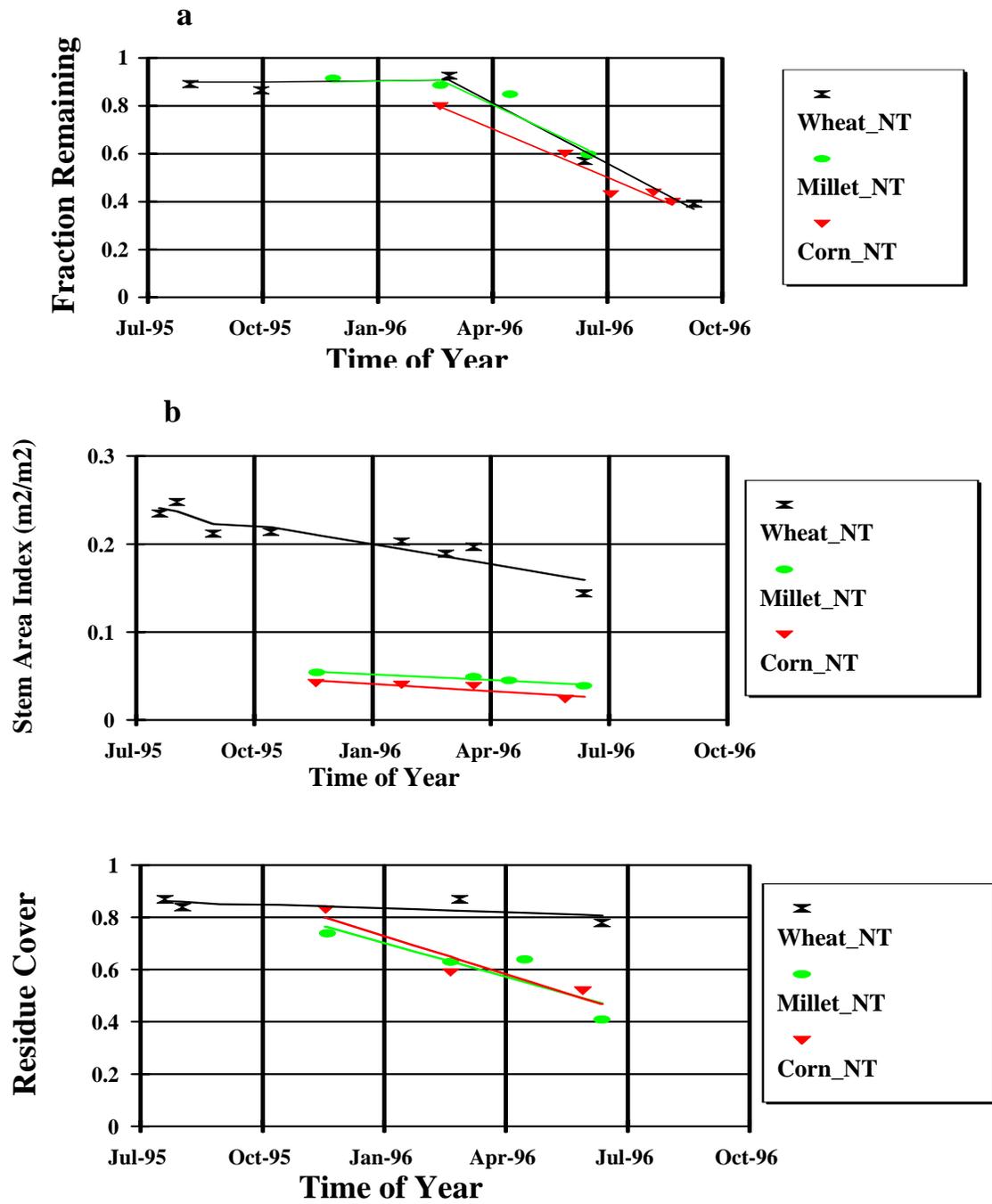
Figure 4. Dynamic residue geometry during a 14 month fallow period, depicting a) mass loss of pre-weighed residues, b) persistence of standing stems, and c) fraction of soil covered by surface residues

Simulation results and field observations indicate residue cover and standing stems alter evaporative demand and microclimate conditions. In turn, residue temperature and water status can affect residue decomposition, driving changes in architecture. Surface energy modules can provide environmental boundary conditions to modules simulating dynamic surface residue decay processes.

Simulation Predictive Accuracy

Non-calibrated simulation of energy balance for wheat_NT, corn_NT, sunflower_NT and wheat_SM systems demonstrate predicted net radiation and surface temperature correspond to field measurements (Table 2). Systematic deviation from observations indicate conceptual or parameterization error in the simulation runs.

Table 2 Linear Regression, PENFLUX Calculations on Field Observations						
Crop Residue*	Net Radiation			Soil Temperature (5 mm)		
	Intercept	Slope	R^2	Intercept	Slope	R^2
Wheat_SM	-11.9	0.95**	0.99	- 3.87	1.36**	0.92
Wheat_NT	-15.8	0.81**	0.99	0.18	0.93**	0.96
Corn_NT	- 8.5	1.00	0.99	- 2.18	1.19**	0.95
Sunflower_NT	4.1	1.14**	0.99	-11.26	1.80**	0.86

*Stubble mulch (SM) and no till (NT) residue management systems; data not available for Millet_NT system.
** Significant difference from 1.00 at 0.01 probability level

Net radiation is a significant driver of sensible and latent (evaporative) heat exchange. Similar patterns of net irradiance occurred for the four soil-residue systems (Figure 5), despite differences in geometry (Table 1). Predictive accuracy was greatest for corn_NT and wheat_SM; a negative bias under radiative loading persisted for wheat_NT, while a positive bias resulted for sunflower_NT residue. We attribute this bias to radiation absorbed by standing stems, which is not quantified in the current model formulation.
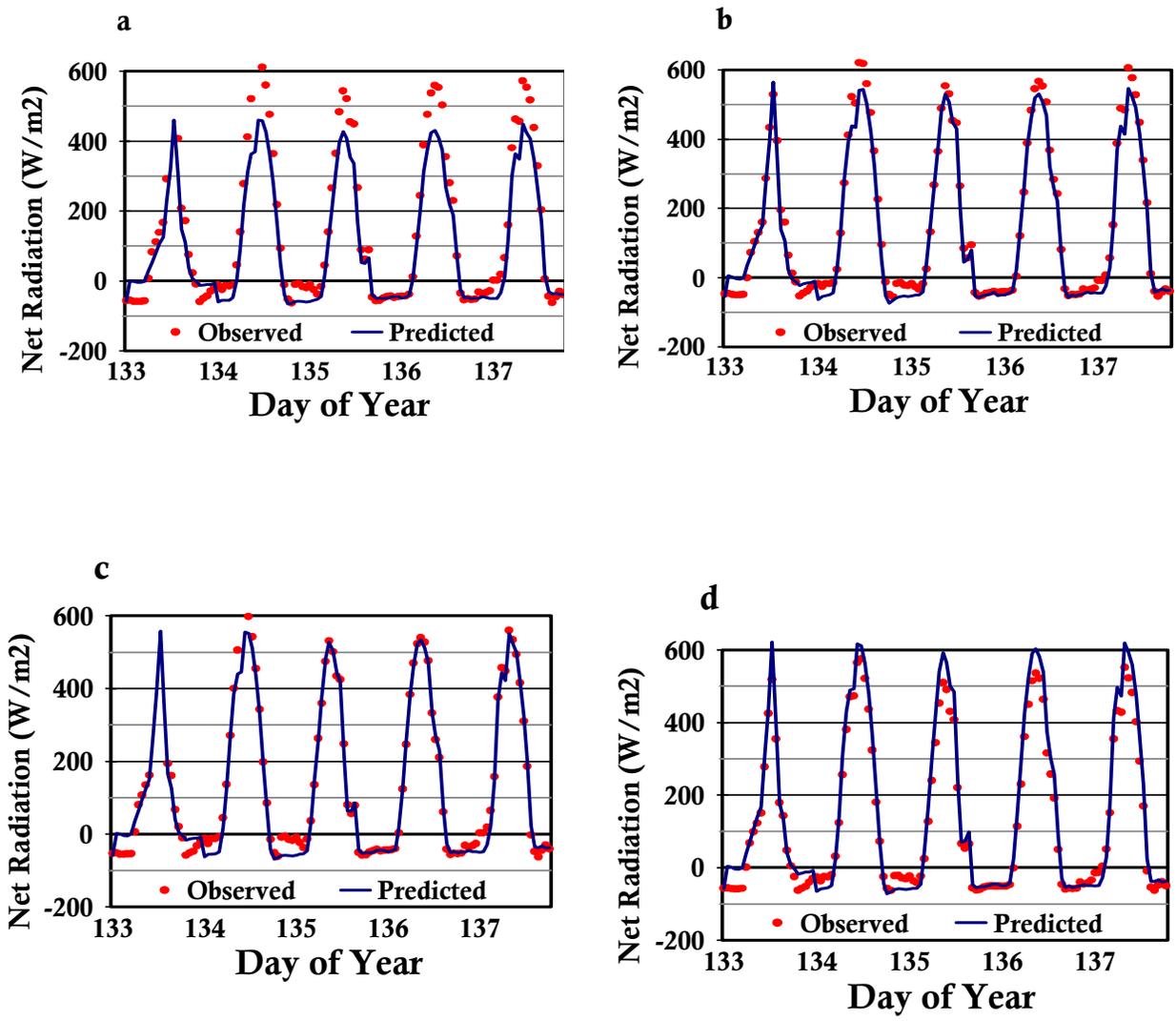
Figure 5. Net radiation observed and calculated by PENFLUX energy balance module for soil-residue systems comprised of a) wheat_NT, b) wheat_SM, c) corn_NT, and d) sunflower_NT.

Surface soil temperatures are sensitive to radiative and convective exchange processes (Equation 1). The timing of temperature fluctuations coincided for predictions and measurements (Figure 6), with greater predictive accuracy for corn_NT and wheat_NT. A positive predictive bias was greater for sunflower_NT and wheat_SM. We attribute this bias to incorrect parameterization of convective properties. Lower soil temperatures observed for sunflower_NT and wheat_SM systems, for which turbulent mixing of air is expected, indicate close coupling of soil and atmospheric thermal conditions. This type of error could result from a positive bias in simulated aerodynamic resistance--quantified by displacement height and roughness length parameters of the theoretical wind speed profile.
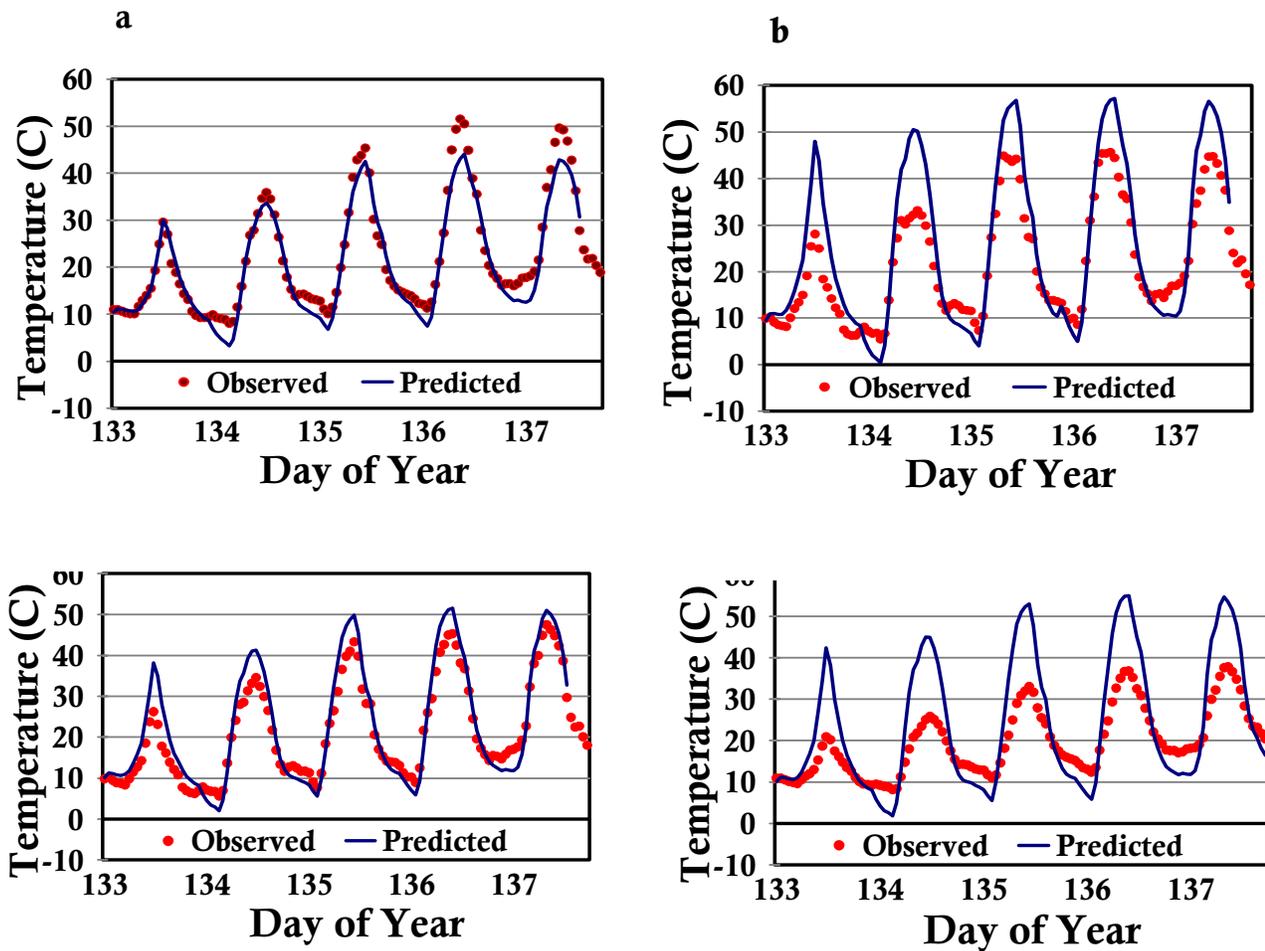
Figure 6. Soil temperature (5 mm) observed and calculated by PENFLUX energy balance module for soil-residue systems comprised of a) wheat_NT, b) wheat_SM, c) corn_NT, and d) sunflower_NT.

Residue impacts on soil water evaporation are illustrated in Figure 7, as simulation by the PENFLUX module of Root Zone Water Quality Model. Simulated evaporation is greatest with sunflower_NT and wheat_SM. Flat residues reduce evaporation by shading the soil from the drying sun. Standing stems insulate the soil from drying winds. Wheat_NT stubble provides greater protection from evaporation than sunflower_NT and millet_NT residues. Residue geometry can modify surface temperature dynamics, affecting the partition of net irradiance to evaporation of soil water. Quantitative knowledge of these processes can support residue management decisions for conservation of soil and water.
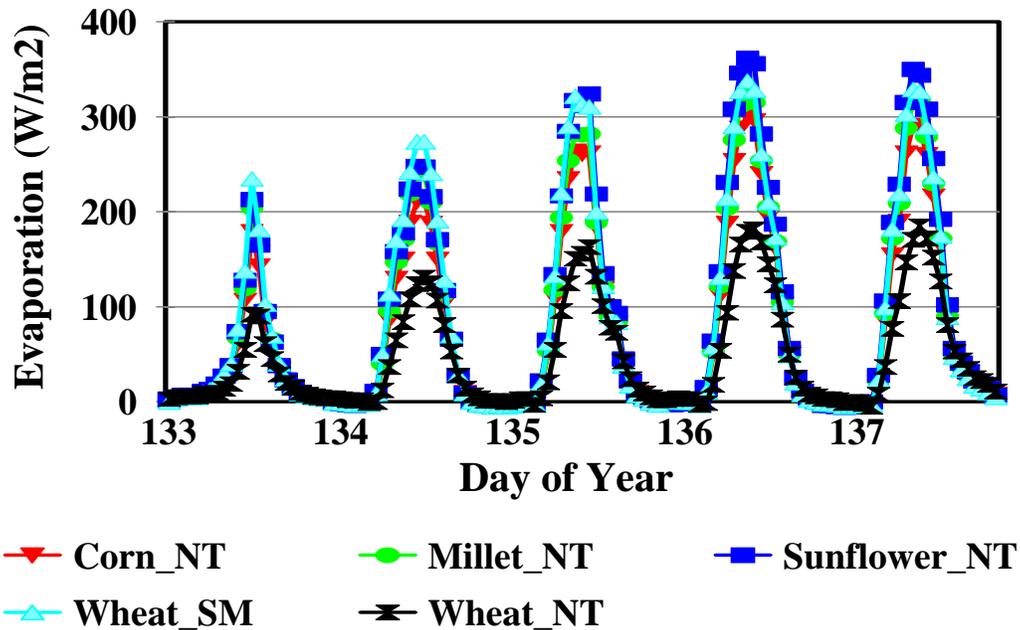
Figure 7. Simulated soil water evaporation as affected by corn_NT, sunflower_NT, wheat_NT and wheat_SM soil residue systems.

Applications for energy balance modules such as PENFLUX include assessment of soil water status and biological development of plants and crop pests. The biases in radiative and convective transfer processes identified here would affect predictions of soil water evaporation during first phase, or energy-limiting evaporation, but become minimal during second phase, or soil-limiting evaporation. For example, the greater degree of convective mixing, indicated for wheat_SM and sunflower_NT, is expected to increase sensible and evaporative heat transfer from the soil surface (Van Duin, 1956). Accelerated evaporation rates would hasten the onset of second phase evaporation. Biases in evaporation predictions are expected to be greatest with wet soil conditions--diminishing to zero at the onset of second phase evaporation. Predictions of cumulative evaporation during extended drying cycles are expected to have minimal bias as this quantity is limited by soil water holding capacity, rather than relative evaporation rates.

Model predictions should be adequate to guide residue/tillage management decision because biases in cumulative evaporation diminish during soil drying cycles. However, simulation of biological processes such as seedling emergence or pest population dynamic could be compromised by error propagation during first phase evaporation. Currently, work is underway to correct biases in radiative and convective processes identified in this effort.

References

Aiken, R.M., G.N. Flerchinger, H.J. Farahani, and K.E. Johnsen. 1997. Energy balance simulation for surface soil and residue temperatures with incomplete cover. Agron. J. 89:404-416.

Bristow, K.L. 1987. On solving the surface energy balance equation for surface temperature. Agric. For. Meteorol. 39:49-54.

Bristow, K.L. and D.G. Abrecht. 1989. The physical environment of two semi-arid tropical soils with partial surface mulch cover. Aust. J. Soil Res. 27:577-587.

Farahani, H.J. and D. DeCoursey. Evaporation and transpiration processes in the soil-residue-canopy system. *In* Root Zone Water Quality Model. RZWQM Development Team (eds.) Water Resources Publ. Highlands Ranch, CO. pp 43-74. (In Press)

Hagan, L.J. and D.V. Armbrust. 1994. Plant canopy effects on wind erosion saltation. Trans. ASAE. 37(2):461-465

Lascano, R.J., R.L. Baumhardt, S.K. Hicks, and J.L. Heilman. 1994. Soil and plant water evaporation from strip-tilled cotton: Measurement and simulation. Agron. J. 86:987-994.

Lyles, L., and B.E. Allison. 1976. Wind erosion: The protective role of simulated standing stubble. Trans. ASAE 19:62-64.

Nielsen, D.C., and S.E. Hinkle. 1994. Wind velocity, snow and soil water measurements in sunflower residues. Great Plains Agric. Council Bull. 150:93-100.

Raupach, M.R. 1992. Drag and drag partition on rough surfaces. Boundary-Layer Meteorol. 60:375-395.

Steiner, J. L., H.H. Schomberg, C.L. Douglas, Jr., and A.L. Black. 1994. Standing stem persistence in no-tillage small-grain fields. Agron. J. 86:76-81.

Van Doren, D.M., Jr. and R.R. Allmaras. 1978. Effect of residue management practices on the soil physical environment, microclimate, and plant growth. p. 49-83. *In* W.R. Oschwald (ed.) Crop residue management systems. ASA Spec. Publ. 31. ASA, CSSA, and SSSA, Madison, WI.

Van Duin, R.H.A. 1956a. On the influence of tillage on conduction of heat, diffusion of air and infiltration of water in soil. Reports of Agric. Invest. No. 62.7 Netherland Ministr. Of Agric., Fisheries & Food Supply, The Hague.

Vigil, M and D. Sparks. 1995. Factors affecting the rate of crop residue decomposition under field conditions. Conservation Tillage Fact Sheet #3-95. USDA-ARS, USDA-NRCS.